Stress orientation, pore pressure and least principal stress in the Norwegian sector of the North Sea

Balz Grollimund[1], Mark D. Zoback[1], David J. Wiprut[1] and Linn Arnesen[2]

[1]*Department of Geophysics, Stanford University, Stanford, CA 94305, USA (e-mail: balz@geo.stanford.edu, zoback@geo.stanford.edu, wiprut@geo.stanford.edu)*

[2]*Research Center, Norsk Hydro ASA, Sandsliveien 90, N-5020 Bergen, Norway (e-mail: Linn.Arnesen@nho.hydro.com)*

ABSTRACT: We have compiled data on stress orientation, pore pressure and least principal stress from over 300 wells in the Norwegian sector of the North Sea. Well-defined regional variations are observed in all three parameters. Incorporation of precise stress orientation data from drilling-induced tensile borehole wall fractures shows that the orientation of maximum horizontal stress is approximately E–W between 60°N and 62°N but tends to be NNW–SSE south of 58°N, similar to the average stress direction seen throughout Great Britain and continental NW Europe. We believe this rotation is due to the superposition of plate-driving stresses with those associated with lithospheric flexure caused by deglaciation. Regional variations of the magnitude of the least principal stress and pore pressure also appear to support the hypothesis that the stress field in this region has been strongly affected by deglaciation.

KEYWORDS: *stress analysis, North Sea, well data, pore pressure, Viking Graben*

INTRODUCTION

In recent years it has become clear that knowledge of the *in situ* stress field is important to address problems as diverse as wellbore stability, hydrocarbon migration and fluid flow through fractured reservoirs. Having good knowledge about the *in situ* stress field and its spatial variations is also crucial to understand geodynamic processes such as ridge push or deglaciation and their influence on the evolution of an area such as the North Sea. To date, knowledge of stress in the North Sea is mostly limited to stress orientations, whereas studies of stress magnitudes in the area have been limited to specific hydrocarbon reservoirs. The aim of this work was therefore to provide a comprehensive understanding of stress in the Norwegian sector of the North Sea, including spatial variations of orientations and magnitudes.

The World Stress Map (WSM) project (Müller *et al.* 1992; Zoback 1992) has accumulated a large database on the orientation of the maximum horizontal stress (S_{Hmax}) including data for the North Sea (Fig. 1). We have used the data from the WSM together with S_{Hmax} orientations obtained from tensile fractures along the wellbore wall to compile a map of S_{Hmax} orientations.

Numerous authors have analysed leak-off tests to determine the least principal stress (S_3) for specific hydrocarbon fields (e.g. Borgerud & Svare 1995; Jorgensen & Bratli 1995), but a comprehensive analysis of S_3 throughout the North Sea has been lacking to date. As pore pressure (P_p) is closely related to stress and affects the faulting behaviour of rock, in this study we have gathered S_3 and P_p information from more than 300 wells, covering most of the Norwegian sector of the North Sea, which enabled us to systematically track magnitudes and spatial changes of S_3 and P_p.

ORIENTATION OF THE MAXIMUM HORIZONTAL STRESS (S_{HMAX})

A number of studies have investigated the stress field in the North Sea by using borehole breakout data to determine the orientation of S_{Hmax} (e.g. Fejerskov 1996; Gölke & Brudy 1996). The breakout data give a good picture of the large-scale changes in stress orientations. However, breakout data are potentially contaminated by keyseating (abrasion of the wellbore wall in deviated wells caused by drill string rotation) and, as a result, the data often reflect the borehole orientation rather than the stress field. Unfortunately, keyseating can occur even at borehole deviation angles of less than 5° from vertical, so a large portion of the breakout data can be affected by keyseating. To clean up the existing breakout database, we excluded all breakouts with azimuths within 10° of the borehole deviation direction. Figure 2 shows the revised breakout data together with S_{Hmax} orientations inferred from drilling-induced tensile fractures.

The bold lines on Figure 2 display the S_{Hmax} orientations of Wiprut & Zoback (1998) as inferred from drilling-induced tensile fractures. Drilling-induced tensile fractures are more reliable to determine the orientation of S_{Hmax} because they are identified from image logs which precludes data contamination of any kind. Importantly, S_{Hmax} orientations from tensile fractures typically show no depth dependence and have a standard deviation of $\pm 10°$ for an entire well (Wiprut & Zoback 1998).

Earthquake focal plane mechanisms can also be used to determine S_{Hmax} orientations (e.g. Bungum *et al.* 1991). However, focal plane solutions give only a rough estimate of the *in situ* stress field, since one has to assume that the principal stress axes form an angle of 45° with the rupture plane. Also, the focal

1354-0793/01/$15.00

plane solutions in the North Sea are not well determined since all the seismographs are onshore and the depth resolution is poor. For these reasons we excluded S_{Hmax} orientations inferred from earthquakes. However, S_{Hmax} orientations from earthquakes generally agree with the borehole measurements.

Figure 2 displays the compilation of available S_{Hmax} orientations from borehole breakouts and drilling-induced tensile fractures. The area between 60°N and 62°N has the best data coverage and roughly shows an E–W direction of S_{Hmax}. A closer examination reveals that S_{Hmax} rotates from an azimuth of *c.* 100° west of the Viking Graben, to *c.* 80° closer to the coast. South of 60°N, S_{Hmax} tends to rotate clockwise to an average direction of *c.* 115° and seems to be independent of longitude. South of 59°N the data coverage is very sparse. The breakout data available for the Central Graben area roughly show NW-striking S_{Hmax} orientations that are subjected to a large scatter. It is noteworthy that S_{Hmax} orientations in the Norwegian sector of the North Sea show no systematic changes with depth. Further, at least for the area between 60°N and 62°N, S_{Hmax} orientations are laterally very consistent and follow clear trends rather than random variations. This implies that the data quality is high enough to reflect changes in the tectonic stress field, and that such changes exist. Finally, the stress orientation data suggest that the stress field in the Norwegian sector of the Northern North Sea deviates from the NNW-striking orientation of S_{Hmax} that is observed almost throughout NW Europe (Müller *et al.* 1992).

MAGNITUDE OF THE LEAST PRINCIPAL STRESS (S_3)

Another valuable source of stress data are leak-off tests (LOT) which give the approximate magnitude of the least principal stress (S_3). A LOT is performed by pressurizing the uncased section of a borehole until fractures open and begin to take in fluid. By plotting the pressure as a function of mud volume pumped into the hole, a deviation from a linear trend indicates the onset of fracture opening and gives a rough estimate for the least principal stress, assuming that the tensile strength of rock is negligible; a good assumption if pre-existing fractures exist. S_3 is fairly well known for a number of oil fields (e.g. Borgerud & Svare 1995; Jorgensen & Bratli 1995). However, a consistent analysis of LOT throughout the entire North Sea was lacking. Thus, we analysed LOT from every borehole displayed in Figure 1 to improve the knowledge of regional trends of the S_3 magnitude at a relatively high resolution.

Assuming that one of the principal stress axes is vertical, the overburden stress (S_v) derived from integrated density logs corresponds to another principal stress magnitude. By looking at S_3 normalized by S_v (S_3/S_v), we can partly determine the stress regime to which a certain area is exposed. In addition to being characteristic of the stress regime the use of S_3/S_v eliminates the effects of varying water depth on stress at a given depth below sea-level. If S_3/S_v is significantly lower than unity, the faulting regime according to Andersonian faulting theory (Anderson 1951) is normal faulting. Conversely, if S_3/S_v is close to unity the faulting regime is more compressive, i.e. strike-slip or even reverse faulting. High S_3/S_v ratios (*c.* 1) can also represent a near-isotropic stress state which may be the case at shallow depths (<1000 m) where the viscous behaviour of the unconsolidated Plio-Pleistocene sediments leads to an almost immediate relaxation of any imposed differential stress. This explains why S_3 on Figure 3 is always very close to S_v at depths shallower than 1000 m. However, analysis of the full stress tensor in the Visund Field (Wiprut & Zoback 1998) shows that, at depths greater than 2000 m below mean sea-level (MSL), the stress state is strongly anisotropic and some faults in the area are close to failure. Similar studies of wellbore failure also show high stress anisotropies at the Fram and Oseberg fields (D. Wiprut pers. comm. 2000). Further, the spatially consistent S_{Hmax} orientations (Fig. 2) require horizontal stress anisotropy and the frequently observed drilling-induced tensile fractures, which are used to constrain many S_{Hmax} orientations on Figure 2, form only under an appreciable horizontal stress anisotropy (Moos & Zoback 1990). Altogether, these observations provide strong evidence for high stress anisotropies at depths greater than 2000 m. Thus, it seems reasonable to assume that S_3/S_v close to unity suggests high horizontal stresses.

We have utilized the following methodology to obtain S_3/S_v ratios for depths between 1500 m and 3000 m at increments of 500 m. First we analysed LOT for 324 vertical exploration wells. We ignored data from production wells to prevent the influence of S_3 changes due to production-related pore pressure drawdown. The obtained S_3-values were classified into good and poor measurements. A good measurement, has a well-defined leak-off pressure and the pressure build-up during the test exceeds the formation breakdown pressure. In the case of the poor measurements, leak-off pressures are not well defined or were not reached at all. Additionally, in some rare cases we obtained S_3 from Minifrac tests which are more reliable than LOT because only small isolated sections of the formation are pressurized in multiple cycles (e.g. Fig. 3d). We used integrated density logs to obtain S_v for every well containing S_3 data, although the obtained S_v with depth profiles do not vary much throughout large portions of the Norwegian sector. Subsequently, we plotted the obtained S_3 values, together with S_v as a function of depth. In cases where one well did not provide enough data we merged nearby wells. Figure 3 shows examples of such stress versus depth plots. We then fit a line through the S_3 data by hand, giving the preference to good LOT measurements and Minifrac tests if available. Since LOT tend to overestimate S_3 (e.g. Gaarenstroom *et al.* 1993), we gave preference to lower S_3 estimates if multiple values were available (e.g. Fig. 3f). As can be seen on Figure 3, not every well provides S_3 data for the entire depth range, but the combination of all available wells allows a very good data coverage of the depth range between 1500 m and 3000 m. To map spatial changes of stress we have plotted S_3/S_v at the previously mentioned depths for areas with satisfactory data coverage (Fig. 4).

To estimate the error associated with the S_3/S_v values we need to consider the uncertainties of the S_3 and S_v measurements. We mentioned earlier that LOT are only an approximate measure of S_3 since they can be affected by several factors, such as a poor cement bond at the casing shoe and a finite tensile strength of the formation. However, Figure 3 shows that the LOT define clear trends of S_3 with depth and are subjected to a maximum scatter of *c.* ±2 MPa. The S_v estimations from integrated density logs are very accurate and overlap for nearby wells. Thus, it is fair to assume that S_v does not scatter more than ±0.5 MPa. Using equation (1) from basic error propagation theory, the error of S_3/S_v can be estimated.

$$\Delta(S_3/S_v) = \left|\frac{\Delta S_3}{S_3}\right| + \left|\frac{\Delta S_v}{S_v}\right| \quad (1)$$

$\Delta(S_3/S_v)$ is the uncertainty of S_3/S_v; ΔS_3 and ΔS_v are the scatter associated with the measurements of S_3 and S_v respectively. $\Delta(S_3/S_v)$ varies with depth since it depends on S_3 and S_v. For a depth of 3000 m, $\Delta(S_3/S_v)$ is approximately 0.05 but gradually increases towards the surface and reaches a value of

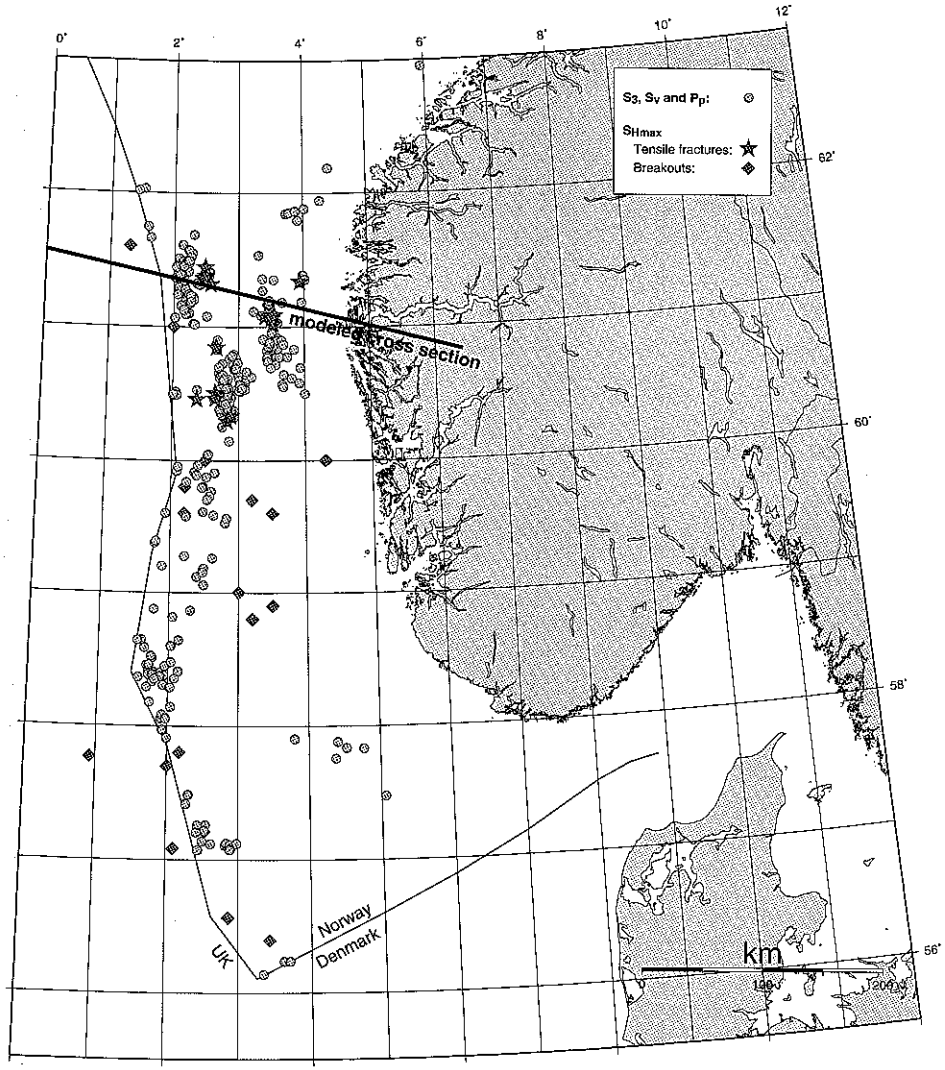

Fig. 1. Data coverage for this analysis. Grey circles: boreholes with leak-off test (S_3), density log (S_v) and pore pressure data. The data coverage is noticeably better north of 60°N than further to the south. The stars indicate the location of boreholes for which Wiprut & Zoback (1998) used tensile fractures to deduce the orientation of S_{max}. The diamonds are the locations of S_{max} measurements from breakouts. The modelled cross-section refers to the model shown in Figure 6.

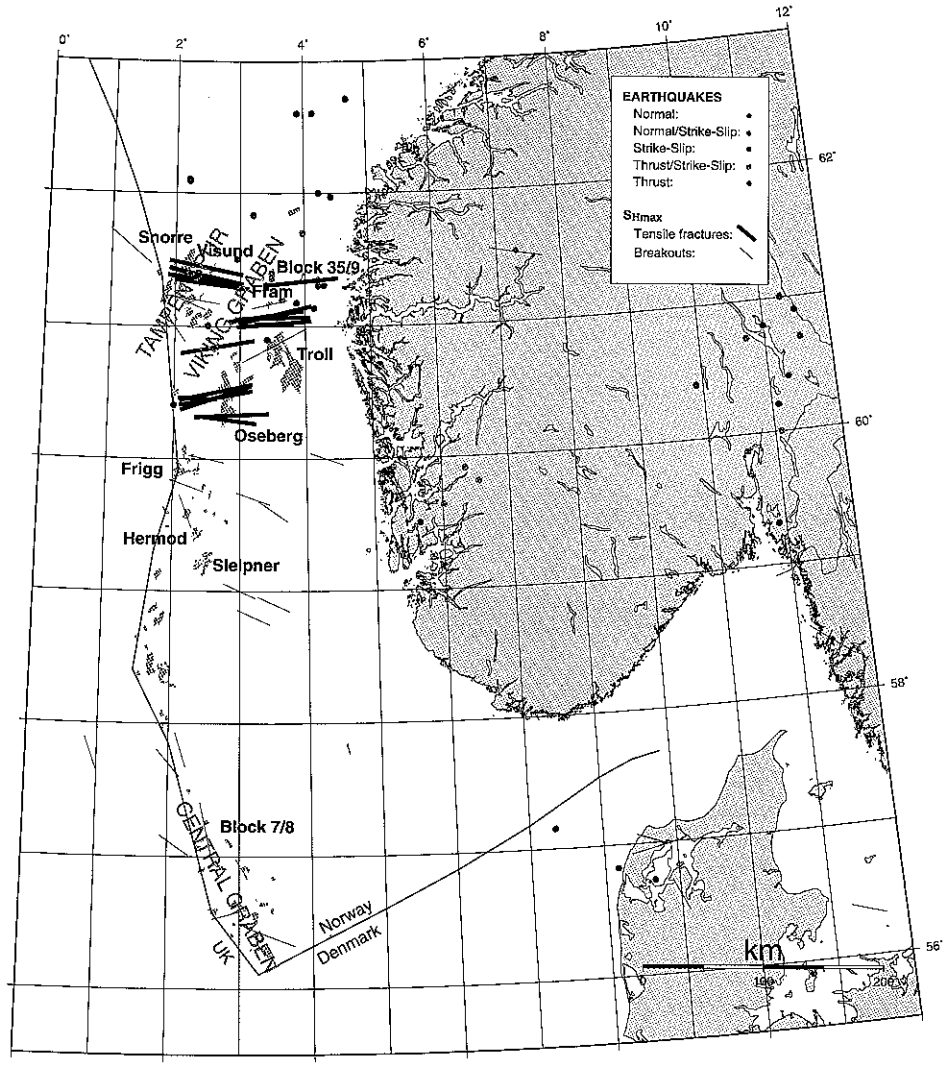

Fig. 2. Compilation of S_{max} orientations in the Norwegian sector of the North Sea from the analyses of breakouts and tensile fractures. The data show that between 60°N and 62°N S_{max} strikes WNW–ESE west of the Viking Graben and rotates to a WSW–ENE striking direction towards the Norwegian coast. Between 59°N and 60°N S_{max} is WNW-orientated. South of 58°N the S_{max} directions are not as well defined as further north but have an average strike of NNW-SSE. Also, the figure shows an increased occurrence of earthquakes north of 60°N.

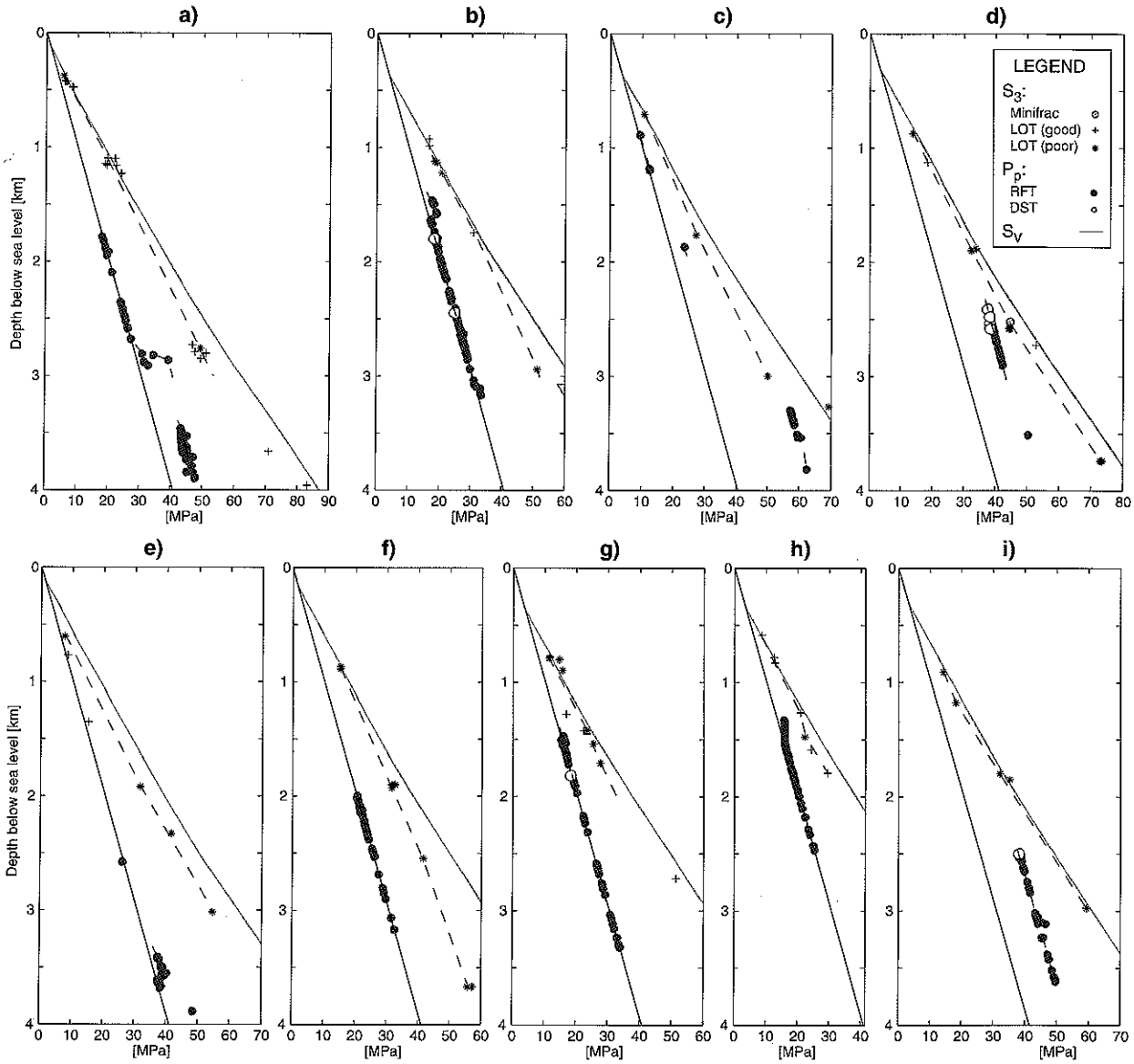

Fig. 3. The different panels (a–i) show typical examples of compiled S_3 and pore pressure data as a function of depths used in the analysis.

0.1 at 1500 m. Also, the data coverage shown on Figure 1 is best between 60°N and 62°N and decreases towards the south, so the values illustrated in Figures 3–5 tend to be more reliable in the Viking Graben area with a decreasing reliability towards the south.

At a depth of 1500 m MSL (Fig. 4a) no clear pattern of lateral stress variation can be observed. However, a zone of relatively low S_3/S_v values (*c.* 0.83) starts to develop around 61.5°N and 4°E. The rest of the Norwegian sector exhibits fairly high S_3/S_v ratios between 0.9 and 1, except for the area surrounding the Frigg Field (see Fig. 2 for locations), which shows slightly reduced S_3/S_v ratios of <0.9. A clearer picture unfolds at 2000 m MSL (Fig. 4b), where S_3/S_v ratios consistently drop close to the coast, reaching values of as low as 0.78 in Block 35/9. Towards the west S_3/S_v gradually increases across the Viking Graben and exhibits values close to unity in the Tampen Spur area. The transition from low S_3/S_v values in Block 35/9 to the highest S_3/S_v ratios in the Tampen Spur occurs over a horizontal distance of *c.* 100 km. Further to the south, S_3/S_v is mostly high and rarely drops below 0.9. At 2500 m MSL (Fig. 4c) the S_3/S_v distribution looks very similar to that of 2000 m MSL. However, the zone of decreased S_3/S_v seems to extend further to the west in the Oseberg region. In the southern parts of the Norwegian sector (south of 60°N), S_3/S_v is generally higher than at 2000 m MSL and never falls below 0.95. The stress distribution at 3000 m MSL has a decreased reliability, because the amount of S_3 data is reduced for this depth slice. Nevertheless, the horizontal stress changes at 3000 m MSL are comparable to the shallower depth slices with high S_3/S_v values (0.9–1) in the west and decreased S_3/S_v closer to the coast. A marked decrease of S_3/S_v occurs in the Oseberg area but around Block 35/9 S_3/S_v is higher than at shallower depth.

In summary, S_3/S_v is consistently high (0.9–1) at distances larger than *c.* 100 km from the coast at all depths, indicating a strike-slip or even reverse faulting stress state. Closer to the coast (between 60°N and 62°N where data are available), S_3/S_v drops to values as low as 0.73 in Block 35/9 at a depth of 2500 m MSL which suggests that the stress state is strike-slip or even normal faulting. Importantly, lines of equal S_3/S_v run roughly parallel to the coast line, which gives some indications as to what causes these lateral stress variations (see discussion section). Earthquake focal plane mechanisms confirm the

transition from reverse faulting offshore to strike-slip or even normal faulting towards the coast for the area between 61°N and 62°N (Lindholm *et al.* 1995).

In contrast to S_3 and S_v, it is much harder to get reliable values for the magnitude of the maximum principal stress (S_1) and analyses of the full stress tensor from wellbore failure are needed. To date, only two studies of the full stress tensor inferred from wellbore failure exist for the North Sea (Wiprut & Zoback 1998; Brudy 1998). Unfortunately, both of these papers deal with fields on the Tampen Spur, so it is impossible to directly track lateral changes of S_1 outside the Tampen Spur. Nevertheless, the results of the two studies are consistent and give values for S_1/S_v between 1.2 and 1.35. Combined with the leak-off data (S_3/S_v=*c.* 0.95) this implies a strike-slip or almost reverse faulting stress regime in the Tampen Spur.

PORE PRESSURE (P_p)

To identify the stress field it is crucial to know the pore pressure since stress and pore pressure are closely related via poroelastic responses (e.g. Engelder & Fischer 1994). Also, the faulting behaviour of rock depends on the stress state and the pore pressure. Thus, we have compiled pore pressure (P_p) data from 385 exploration wells in the Norwegian sector of the North Sea. We ignored data from production wells to prevent the influence of production-related pore pressure drawdown. The pore pressures are derived from repeat formation tests (RFT), which are routinely performed at reservoir depth. An RFT is carried out by measuring the fluid pressure necessary to prevent flow into or out of the formation. Additionally, a limited number of P_p values come from drill stem tests. Almost all P_p measurements are made in sandstones, so the subsequent analysis resembles P_p as observed in sandstones. We produced maps of overpressure ($P_p - P_{hydrostatic}$) for different depth slices in the same way as for S_3/S_v ratios to track changes of P_p both laterally and with depth. The error associated with the P_p measurements used in this analysis is negligible. However, the methodology of showing regional trends of P_p (Fig. 5) does not resolve P_p-variations within a specific hydrocarbon reservoir. For reasons of data confidentiality we cannot provide absolute P_p values in Figure 5.

At depths shallower than 1500 m MSL the pore pressure is hydrostatic throughout the Norwegian sector of the North Sea, which is not surprising since the pore fluids are likely to be in hydraulic communication with the sea floor. A small zone of moderate overpressure starts to develop south of 58°N at 1500 m MSL (Fig. 5a). The pore pressures in the remaining parts of the Norwegian sector are, however, close to hydrostatic. At 2000 m MSL (Fig. 5b) a distinct zone of hard overpressure starts to develop in the Tampen Spur. Additionally, a small zone of overpressure exists in the vicinity of Block 35/9. The previously mentioned zone of overpressure at 1500 m MSL south of 58°N still exists at 2000 m MSL. However, the majority of the Norwegian sector exhibits pore pressures close to hydrostatic at 2000 m MSL. At 2500 m MSL (Fig. 5c) the zone of hard overpressure in the Tampen Spur area is even more pronounced. In contrast to the pattern at 2000 m MSL, at 2500 m MSL the zone of elevated pore pressures around Block 35/9 has disappeared and, except for the Tampen Spur area, most of the Norwegian sector exhibits hydrostatic pore pressures. Figure 5d shows that the Tampen Spur still is strongly overpressured at 3000 m MSL. However, further south in the vicinity of the Frigg and Hermod fields a very strong overpressure can be observed. Also, the area south of 59°N generally displays a slight overpressure at 3000 m MSL. Still, large parts of the Norwegian sector show pore pressures close to hydrostatic, including the areas surrounding the Troll and Oseberg fields.

In summary, pore pressures are mostly hydrostatic throughout the Norwegian part of the North Sea to a depth of 2500 m MSL, with the exception of the Tampen Spur, Blocks 35/9 and 7/8. The Tampen Spur shows the most marked pore pressure increase, whereas the overpressure in Block 35/9 is small and limited to a relatively small depth interval.

DISCUSSION

By comparing the orientations of S_{Hmax} with S_3/S_v between 60°N and 62°N (Figs 2 and 4), it is striking that S_{Hmax} generally rotates where S_3/S_v is low. Roughly speaking, the area east of the Viking Graben (e.g. Oseberg, Troll, 35/9) shows anomalous S_{Hmax} orientations (*c.* 80° instead of the regionally typical >100°) and S_3/S_v drops to less than 0.8 in the same region. This close spatial relationship between the S_{Hmax} rotation and the S_3/S_v decrease suggests that both are caused by the same mechanism.

Possible sources of spatial stress variations

Stein *et al.* (1989) have discussed a number of possible sources of stress perturbations for the Baffin Bay region in northeastern Canada, which is comparable to the Norwegian coast since both are formerly glaciated, passive continental margins. Numerous authors have pointed out the importance of ridge push as a large-scale stress source along the Norwegian margin (Müller *et al.* 1992; Lindholm *et al.* 1995). Since the crust cools down and becomes denser as it moves away from the Mid Atlantic Ridge, gravitational sliding occurs and causes increased horizontal stresses in the direction of plate motion. Thus, ridge push is likely to be the source of the general S_{Hmax} orientation, but the local rotation of S_{Hmax} orientations between 60°N and 62°N and the associated change in horizontal stress magnitudes must have another origin. Artyushkov (1973) has calculated stress perturbations resulting from the transition of continental to oceanic crust. Since the continental crust has a lower density with respect to the mantle it tends to spread out towards the oceanic crust. However, since the continental margin is located *c.* 100 km northwest of the Tampen Spur we would expect decreased horizontal stresses everywhere between 61°N and 62°N, with a tendency for increasing rather than decreasing stress magnitudes towards the coast. A further source of stress perturbation might be the rapid sedimentation that took place during the Tertiary and especially during the Plio-Pleistocene. Sediment thicknesses of up to 1 km accumulated during Tertiary times, causing a significant load on the lithosphere (Doré 1992). As a result, the lithosphere bends under the sediment load, which leads to an increase of the horizontal stresses at shallow crustal depth in areas of high sedimentation (e.g. Tampen Spur). Hence, lithospheric bending due to sedimentation might explain the observed spatial stress variations. However, the expected lateral stress variation would be rather smooth, whereas observed stress variations show an abrupt change across the Viking Graben. Also, sedimentation occurs over a relatively long time period (10^6 years) and relaxation processes within the crust might have markedly reduced the initial stress perturbations due to sedimentation.

The influence of deglaciation on stress

Lastly, an obvious source of stress variation along the Norwegian coast is lithospheric flexure associated with the

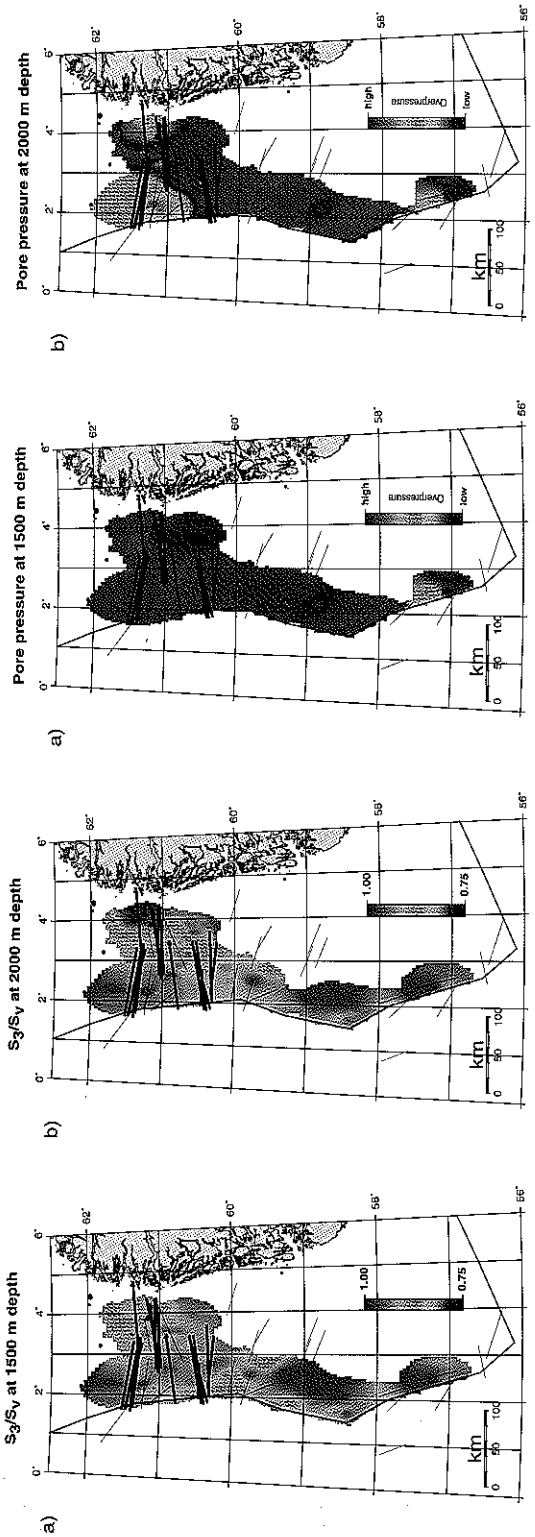

Fig. 4. Lateral variation of the least principal stress normalized by the vertical stress (S_3/S_V) for different depth slices. S_3 is derived from leak-off tests and S_V comes from integrated density logs. The figure shows that S_3/S_V is consistently low close to the Norwegian coast and increases towards the west (perpendicular to the coast line). The black lines indicate S_{max} orientation from Figure 2.

Fig. 5. Lateral variation of overpressure for different depth slices. The overpressure is mostly derived from RFT-logs and in some cases from drill stem tests. The figure shows that the pore pressure is mostly hydrostatic, but highly overpressured west of the Viking Graben (Tampen Spur). Slight overpressure also occurs south of 58°N. The black lines indicate S_{max} orientations from Figure 2.

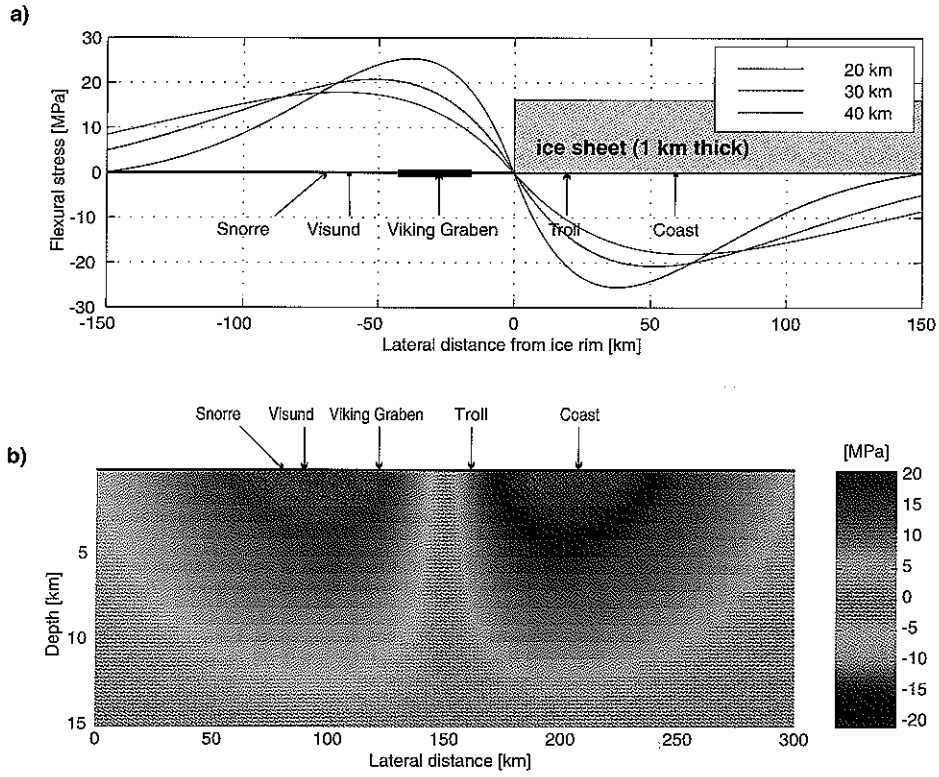

Fig. 6. Predicted stress perturbation for deglaciation on an elastic lithosphere with an initially isotropic stress state. (a) Predicted stress perturbations at the surface for different effective elastic thicknesses of the lithosphere. For lithospheric thicknesses between 30 and 40 km the maximum stress increase is *c.* 20 MPa and occurs in the fields on the Tampen Spur (e.g. Snorre, Visund). Similarly the maximum stress decrease is *c.* −20 MPa and is located close to the coast. (**b**) Predicted stress changes for an elastic lithospheric thickness of 30 km as a function of depth. Stress perturbations decrease monotonically to a depth that corresponds to half the plate thickness (15 km). Below this depth the stress perturbation would be similar but with opposite signs.

melting of the late Weichselian ice sheet. Assuming that the stress field was laterally uniform before the onset of ice melting, the isostatic response due to deglaciation and the resulting lithospheric flexure leads to a horizontal stress decrease in areas which were formerly covered by ice and to a horizontal stress increase at shallow depth away from the former ice sheet.

If the lateral ice sheet extent at 15 000 Ma as given by Mangerud *et al.* (1979) is representative for most of the ice sheet's history, the Tampen Spur is expected to have increased horizontal stress magnitudes. Conversely, the region east of the Viking Graben would be subjected to a stress decrease. Figure 6 shows expected stress perturbations as a result of deglaciation for an elastic lithosphere (Turcotte & Schubert 1982). This analytical model assumes that the shape of the ice sheet can be described by a step function and that the ice sheet was 1 km thick. Figure 6a shows predicted stress perturbations in an east–west direction at the surface for different effective elastic lithospheric thicknesses. The model shows that for effective elastic thicknesses between 30 and 40 km the half-wavelength of the stress variation is around 100 km, which matches the observed stress variation between 60°N and 62°N. For the fields in the Tampen Spur (e.g. Snorre, Visund) the model predicts an east–west stress increase of the order of 20 MPa near the surface. Since this stress increase is perpendicular to the ice sheet margin it leads to a more pronounced orientation of S_{Hmax}. Closer to the coast the east–west stress is predicted to decrease by about 20 MPa, possibly leading to the observed rotation of S_{Hmax}. Figure 6b shows that the predicted stress perturbation decreases with depth and disappears at a depth corresponding to half the effective lithospheric thickness. However, these predicted stress perturbations are upper bounds, since we assume that no spatial stress perturbations existed before the onset of ice melting. Further, gravity and uplift data show that the rebound is incomplete (Ekman & Makinen 1996), so the lithosphere is not yet subjected to the full amount of bending. Nevertheless, the lateral extent and, roughly, the magnitudes agree with the observed stress variations. Finally, it is striking that the area between 60°N and 62°N – the region of the largest horizontal stress variations – shows a remarkably increased seismic activity (Fig. 2). This strongly suggests that the mechanism causing the previously described stress variations is also responsible for triggering the earthquakes in this province.

The influence of deglaciation on pore pressure

Figures 4 and 5 show that high pore pressures in the Tampen Spur coincide with high S_3/S_v ratios, whereas decreased stresses closer to the coast (e.g. Block 35/9) are associated with low, close to hydrostatic, pore pressures. This close relationship between stress and pore pressure suggests that they are connected via a close cause–effect relation. Engelder & Fischer (1994) have shown that S_3 drops in response to pore pressure drawdown in numerous hydrocarbon provinces. As a result of such a poroelastic response, S_3 within the hydrocarbon reservoir decreases by *c.* 70% of the associated pore pressure drop. Since S_3 seems to follow the pore pressure, the high observed S_3 in the Tampen Spur could be induced by high pore pressures. However, if that was the case, stress magnitudes south of 61°N should be lower than observed because the pore pressure is mostly hydrostatic. But, if pore pressure-changes influence S_3, S_3 changes might, in turn, have an effect on the pore pressure. So, maybe at least part of the high observed pore pressures in the Tampen Spur result from a poroelastic response to the increase of horizontal stresses. In other areas (e.g. south of the Tampen Spur), where horizontal stresses are as high as in the Tampen Spur, the induced pore pressure increase might have simply leaked away. Consequently, the high pore pressures in the Tampen Spur might be partially the result of a poroelastic response to increased stress magnitudes due to deglaciation. Closer to the coast, where deglaciation is expected

to decrease horizontal stress, poroelasticity would lead to subhydrostatic pore pressures, which does not match the observation of more or less hydrostatic P_p. However, a stress decrease also tends to cause faulting, which in turn increases permeability (Barton *et al.* 1995). As a result of increased permeability the pore fluids communicate with the sea floor and no subhydrostatic pore pressure can develop.

Several other processes, such as under-compaction and hydrocarbon maturation, have certainly influenced pore pressures in the North Sea (Caillet *et al.* 1991). For instance, zones of moderate overpressure occur south of 58°N in the Norwegian sector and close to the Norwegian coast at 61.2°N, where deglaciation does not lead to a horizontal stress increase and, therefore, cannot be explained by a poroelastic response to deglaciation.

CONCLUSIONS

We conclude that *in situ* stress and pore pressure in the Norwegian sector of the North Sea are regionally consistent and follow well-defined spatial trends. The most marked change of stress occurs between 60°N and 62°N. In this area the horizontal stresses are relatively low close to the coast and increase further offshore at distances greater than *c.* 100 km from the coast. This change of stress magnitude is accompanied by a rotation of S_{Hmax} of *c.* 20°. A simple model of elastic plate flexure suggests that the observed stress variations are the result of deglaciation. The pore pressure is close to hydrostatic in most of the Norwegian sector, except for the area west of the Viking Graben, north of 61°N where large overpressures exist at depths greater than 1500 m. These high pore pressures west of the Viking Graben might partly be caused by deglaciation.

We would like to thank Norsk Hydro for generously providing the data and financial support for this study.

REFERENCES

Anderson, E. M. 1951. *The Dynamics of Faulting and Dyke Formation with Applications to Britain.* Oliver and Boyd, Edinburgh.

Artyushkov, E. V. 1973. Stresses in the lithosphere caused by crustal thickness inhomogeneities. *Journal of Geophysical Research*, **78**, 7675–7708.

Barton, C. A., Zoback, M. D. & Moos, D. 1995. Fluid flow along potentially active faults in crystalline rock. *Geology*, **23**(8), 683–686.

Borgerud, L. & Svare, E. 1995. In-situ stress field on the Norwegian Margin, 62°–67° north. *Workshop on Rock Stresses in the North Sea.* SINTEF, Trondheim, Norway, 165–178.

Brudy, M. 1998. Determination of the State of Stress by Analysis of Drilling-Induced Fractures – Results from the northern North Sea. *Eurock*, **1**: Proceedings of the Eurock 98 Conference, Trondheim, Norway. SPE, 141–149.

Bungum, H., Alsaker, A., Kvamme, L. B. & Hansen, R. A. 1991. Seismicity and seismotectonics of Norway and nearby continental shelf areas. *Journal of Geophysical Research*, **96**(B2), 2249–2265.

Caillet, G., Sejourne, C., Grauls, D. & Arnaud, J. 1991. The hydrodynamics of the Snorre Field area, offshore Norway. *Terra Nova*, **3**, 180–194.

Doré, A. G. 1992. The base Tertiary surface of southern Norway and the northern North Sea. *Norsk Geologisk Tidsskrift*, **72**, 259–265.

Ekman, M. & Makinen, J. 1996. Recent postglacial rebound, gravity change and mantle flow in Fennoscandia. *Geophysical Journal International*, **126**, 229–234.

Engelder, T. & Fischer, M. P. 1994. Influence of poroelastic behaviour on the magnitude of minimum horizontal stress, S_h, in overpressured parts of sedimentary basins. *Geology*, **22**, 949–952.

Fejerskov, M. 1996. *Determination of in-situ rock stresses related to petroleum activities on the Norwegian continental shelf.* PhD thesis. Norwegian University of Science and Technology, Trondheim, Norway.

Gaarenstroom, L., Tromp, R. A. J., De Jong, M. C. & Brandenburg, A. M. 1993. Overpressures in the Central North Sea: Implications for trap integrity and drilling safety. *In:* Parker, J. R. (ed.) *Petroleum Geology of Northwest Europe: Proceedings of the 4th Conference.* Geological Society, London, 1305–1313.

Gölke, M. & Brudy, M. 1996. Orientation of crustal stresses in the North Sea and Barents Sea inferred from borehole breakouts. *Tectonophysics*, **266**, 25–32.

Jorgensen, T. & Bratli, R. K. 1995. In-situ stress determination and evaluation at the Tampen Spur area. *Workshop on rock stress in the North Sea.* Trondheim, Norway, 240–249.

Lindholm, C. D., Bungum, H., Villagram, M. & Hicks, E. 1995. Crustal Stress and Tectonics in Norwegian Regions Determined from Earthquake Focal Mechanisms. *Workshop on rock stress in the North Sea.* Trondheim, Norway, 77–91.

Mangerud, J., Larsen, E., Longva, O. & Sonstegaard, E. 1979. Glacial History of Western Norway 15,000–10,000 B.P. *Boreas*, **8**(2), 179–187.

Moos, D. & Zoback, M. D. 1990. Utilization of Observations of Well Bore Failure to Constrain the Orientation and Magnitude of Crustal Stresses: Application to Continental, Deep Sea Drilling Project, and Ocean Drilling Program Boreholes. *Journal of Geophysical Research*, **95**(B6), 9305–9325.

Müller, B., Zoback, M. L., Fuchs, K., Mastin, L., Gregersen, S., Pavoni, N., Stephansson, O. & Ljunggren, C. 1992. Regional patterns of tectonic stress in europe. *Journal of Geophysical Research*, **97**(B8), 11 783–11 803.

Stein, S., Cloetingh, S., Sleep, N. H. & Wortel, R. 1989. Passive Margin Earthquakes, Stresses and Rheology: Earthquakes at North-Atlantic Passive Margins. *In:* Gregersen, S. & Basham, P. W. (eds) *Neotectonics and Postglacial Rebound.* Kluwer, 231–259.

Turcotte, D. L. & Schubert, G. 1982. *Geodynamics.* John Wiley & Sons, New York City.

Wiprut, D. J. & Zoback, M. D. 1998. High horizontal stress in the Visund field, Norwegian North Sea. *Eurock*, 1. Trondheim, Norway, 199–208.

Zoback, M. L. 1992. First- and Second-Order Patterns of Stress in the Lithosphere: The World Stress Map Project. *Journal of Geophysical Research*, **97**(B8), 11 703–11 728.

Received 23 June 1999; revised typescript accepted 6 March 2000